

# Spin blockade in hole quantum dots: Tuning exchange electrically and probing Zeeman interactions

Jo-Tzu Hung,<sup>1</sup> Elizabeth Marcellina,<sup>1</sup> Bin Wang,<sup>1,2</sup> Alexander R. Hamilton,<sup>1</sup> and Dimitrie Culcer<sup>1</sup>

<sup>1</sup>School of Physics, The University of New South Wales, Sydney NSW 2052, Australia

<sup>2</sup>University of Science and Technology of China, Hefei, Anhui, 230026, China

(Received 6 October 2016; revised manuscript received 28 April 2017; published 26 May 2017)

Spin-orbit coupling is key to all-electrical control of quantum-dot spin qubits, and is often much stronger for holes than for electrons. The recent development of high-quality hole nanostructures has generated considerable interest in hole-spin qubit architectures [C. Kloeffel and D. Loss, *Annu. Rev. Condens. Matter Phys.* **4**, 51 (2013)]. Yet hole-spin quantum computing hinges on the ability to discriminate between competing Zeeman terms and on the understanding of the complex interplay between the Zeeman and spin-orbit interactions, which are probed via Pauli spin blockade. Here we investigate spin blockade for two heavy holes in a gated double quantum dot in an in-plane magnetic field  $\mathbf{B}$ . We find that the leakage period as a function of the field orientation is critically dependent on the relative magnitude of Zeeman interaction terms linear and cubic in  $B$ , exhibiting a beat pattern when the two are comparable in magnitude, and providing an effective way to discriminate between the two. Moreover, in certain materials the singlet-triplet exchange splitting is highly tunable by an appropriate choice of field direction, yielding a straightforward control variable for quantum information processing. These findings should stimulate new experiments on hole qubits.

DOI: 10.1103/PhysRevB.95.195316

## I. INTRODUCTION

Spin-based quantum computing platforms relying on hole quantum dots (QDs) have recently attracted considerable attention [1–15]. They allow long spin coherence times and fast electrically driven spin resonance thanks to the strong hole spin-orbit coupling (SOC) [16–25]. Moreover, owing to their effective spin  $J = \frac{3}{2}$ , spin dynamics in hole systems often exhibits physics absent in electron systems [26–31]. The experimental realization of high-quality low-dimensional hole systems has not only opened the door to hole-qubit architectures [32–35], but also advanced the studies of such exotic topics as Majorana fermions [36–38] and artificial graphene [39–41].

Probing the SOC is necessary to achieve fast, low-power single-qubit operations, while probing the hole-hole interaction is important for scaling up quantum computing platforms. Pauli spin blockade (PSB) [42] has been an effective probe for both of these in electron systems [43–45] as well as a mechanism for spin-qubit readout [46,47]. Yet in low-dimensional hole systems the complexity and strong anisotropy of the Zeeman interaction causes significant difficulties [48]. The linear Zeeman coupling to an in-plane magnetic field  $B$  vanishes to a first approximation [27]. In practice it is nonvanishing but typically small, and is strongly affected by SOC [5,9,13,49–54]. An additional Zeeman interaction exists cubic in  $B$  [48,55]. The relative strength of these two is not known *a priori* for individual structures [13,54–59]. The development of hole-spin quantum computing requires a general understanding of the effect of the Zeeman interaction on PSB and a practical method to discriminate between linear and cubic Zeeman terms.

Here we investigate PSB in a gate-defined hole double QD in an in-plane magnetic field. We show that the PSB is periodic in the angle characterizing the field orientation and its periodicity depends strongly on the dominant Zeeman interaction. The PSB can thus serve as a probe of the form and magnitude of the in-plane Zeeman coupling (see Fig. 1). Furthermore, when the SOC is strong, the exchange splitting, a crucial component

of all spin-qubit architectures [60–65], depends sensitively on the magnetic field orientation [see Fig. 2(a)]. We expect these important findings to stimulate and aid the interpretation of state-of-the-art experiments on hole qubits.

In this article we introduce the model Hamiltonian and the effective Hamiltonian for heavy-hole PSB in Sec. II, where the SO-induced tunneling field direction and the exchange splitting are also discussed. In Sec. III we solve the SO-induced leakage current based on the effective Hamiltonian, and present our results in terms of relevant experimental parameters. Section IV discusses experimental applicability and the limitation of our current model. In Sec. V we conclude this work and leave further details in the Appendix.

## II. THEORETICAL FRAMEWORK

The  $J = \frac{3}{2}$  spin, comprising a heavy hole (HH,  $|\frac{3}{2}, \pm \frac{3}{2}\rangle$ ) and a light hole (LH,  $|\frac{3}{2}, \pm \frac{1}{2}\rangle$ ), has a fourfold degeneracy at the band edge  $\mathbf{k} = 0$ . In two-dimensional (2D) hole systems, confinement in the growth direction lifts this degeneracy and cause a splitting between the HH and LH, which is often the largest energy scale ( $> 10$  meV in GaAs inversion layers), whereupon the lowest energy (HH) subband may be described by a pseudospin, a picture we adopt in this work.

We consider a gated HH double dot grown along  $\hat{z} \parallel [001]$  and positioned at  $(x_j, y_j) = (\mp d, 0)$ , where  $j = L, R$  label the left and right dot, respectively. An in-plane magnetic field  $\mathbf{B} = B(\cos \theta, \sin \theta)$  is applied, with  $\theta$  defined from  $\hat{x}$ . The strong SOC is expected to lift the PSB [7,9,12,13], due to the suppressed contact hyperfine interaction [19,21]. We describe the PSB by deriving an effective SO tunneling Hamiltonian between (1,1) and (0,2), with  $(N_L, N_R)$  being the charge state of the  $L$  and  $R$  dots.

The Hamiltonian is  $\hat{H} = \sum_{j=L,R} \hat{H}_d^{(j)} + \hat{H}_Z^{(j)} + \hat{H}_{SO}^{(j)}$ .  $\hat{H}_d^{(j)} = \frac{(\mathbf{p}_j - e\mathbf{A})^2}{2m^*} + \frac{m^*}{2} [\omega_x^2(x - x_j)^2 + \omega_y^2 y^2]$  contains the kinetic energy and parabolic confinement, with  $m^*$  the effective HH mass,  $\mathbf{p}_j$  the canonical momentum,  $\mathbf{A} = zB(\sin \theta, -\cos \theta)$

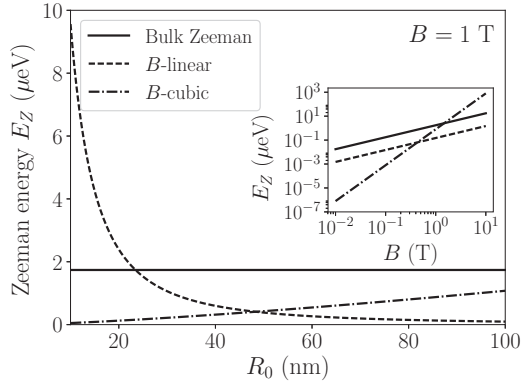


FIG. 1. Contributions to the Zeeman energy of a GaAs hole double QD when  $\mathbf{B} \parallel \hat{x}$ , as a function of the dot radius  $R_0$ : the bulk Zeeman term, and the indirect  $B$ -linear and  $B^3$  couplings. We have included the first  $\hat{z}$  subband with the HH-LH splitting 10 meV. Inset: The contributions for  $R_0 = 80$  nm, with varying  $B$ .

the gauge potential, and  $\hbar\omega_{x/y}$  the confinement energy quantum. The  $j$  dot orbitals are the normalized wave functions of the two harmonic oscillators  $|n_x, n_y^{(j)}\rangle$  along  $\hat{x}$  and  $\hat{y}$ , with  $n_x$  and  $n_y$  the respective quantum numbers. The radii  $R_{0,x/y} \equiv [\hbar/(m^*\omega_{x/y})]^{1/2}$ , and for a circular QD,  $R_{0,x} = R_{0,y} = R_0$ .

The Zeeman Hamiltonian  $\hat{H}_Z^{(j)}$  includes both  $B$ -linear and  $B^3$  terms [66]:

$$\begin{aligned} \hat{H}_Z^{(j)} = & -\frac{3}{2}q\mu_BB(e^{i\theta}\sigma_{j+} + e^{-i\theta}\sigma_{j-}) \\ & -\mu_BB\frac{f}{\hbar^2}(e^{-i\theta}\sigma_{j+}p_{j-}^2 + e^{i\theta}\sigma_{j-}p_{j+}^2) \\ & + (\mu_BB)^3F(e^{-3i\theta}\sigma_{j+} + e^{3i\theta}\sigma_{j-}), \end{aligned} \quad (1)$$

with  $\sigma_j$  the Pauli matrices of the  $j$  pseudospin,  $\sigma_{j\pm} \equiv \frac{1}{2}(\sigma_{jx} \pm i\sigma_{jy})$ , and  $p_{j\pm}$  is the raising (lowering) operators in the momentum. The first term in Eq. (1) is the zeroth-order bulk Zeeman splitting between the  $m_J = \pm\frac{3}{2}$  states, with the

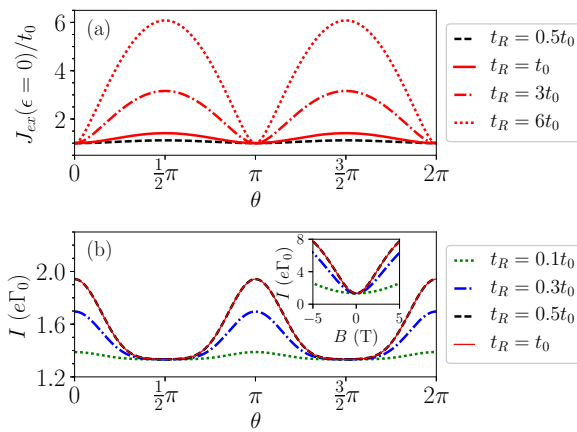


FIG. 2. In a GaAs double QD where  $E_Z \propto B$ ,  $R_0 = 30$  nm and  $t_0 = 200 \mu\text{eV}$ . (a)  $J_{ex}(\epsilon = 0)/t_0$  as a function of  $\theta$  based on Eq. (5), for various values of  $t_R/t_0$ . (b)  $I(\theta)$  at  $B = 1$  T. The  $t_R = 0.5$  and  $t_R = t_0$  curves are overlapping.  $\Gamma_{11} \equiv \Gamma_0 = 3$  MHz, i.e.,  $e\Gamma_0 \approx 0.48$  pA. Inset:  $I(B)$  at  $\theta = 0$  for the same dot geometry.

bulk Luttinger Zeeman parameter  $q$  (e.g.,  $q = 0.01$  for GaAs [66]). The second term is an indirect  $B$ -linear coupling allowed by the symmetry [67], and the third being the indirect  $B^3$  couplings via  $m_J = \pm\frac{1}{2}$  states [66]. The parameters  $f$  and  $F$  are both inversely proportional to the HH-LH splitting (see Appendix A.) These individual contributions to the Zeeman energy are shown in Fig. 1 for a GaAs double QD. As  $R_0$  increases, the indirect  $B$ -linear ( $B^3$ ) term will be reduced (enhanced), and the  $B^3$  term may dominate at large  $B$ .

The single-spin basis is comprised of  $|\uparrow\rangle_{\theta_Z} = \frac{1}{\sqrt{2}}[1, e^{-i\theta_Z}]^T$  and  $|\downarrow\rangle_{\theta_Z} = \frac{1}{\sqrt{2}}[1, -e^{-i\theta_Z}]^T$ , with  $\theta_Z$  subject to the dominating Zeeman term and  $[\dots]^T$  the transpose of a row vector. Focusing on the case where the bulk  $B$ -linear term dominates, we have  $\theta_Z = \theta$  [otherwise,  $\theta_Z = -\theta$  ( $-3\theta$ ) when the indirect  $B$ -linear ( $B^3$ ) term dominates]. We expand the two-spin Hilbert space into the singlet  $|S\rangle = \frac{1}{\sqrt{2}}(|\uparrow\downarrow\rangle_\theta - |\downarrow\uparrow\rangle_\theta)$ , and the unpolarized and two polarized triplet states,  $|T_0\rangle = \frac{1}{\sqrt{2}}(|\uparrow\downarrow\rangle_\theta + |\downarrow\uparrow\rangle_\theta)$ ,  $|T_+\rangle = |\uparrow\uparrow\rangle_\theta$ , and  $|T_-\rangle = |\downarrow\downarrow\rangle_\theta$ . Accordingly, the double-dot Zeeman splitting takes the form  $E_Z = \mu_B B[-3q - \frac{\sqrt{2}f\chi^2}{R_0^2} \cos(2\theta)] + \sqrt{2}F\mu_B^3 B^3 \cos(2\theta)$ . Depending on the values of  $q$  and  $f$  (subject to device details), the two  $B$ -linear terms could be canceled up at certain field orientation; the Zeeman splitting will become cubic in  $B$ , even when we include the next-order bulk Luttinger contribution  $\propto q(\mu_B B)^3$ .

The SOC is given by  $\hat{H}_{\text{SO}}^{(j)} = \hat{H}_{\text{R}}^{(j)} + \hat{H}_{\text{D}}^{(j)}$ , with [18]

$$\hat{H}_{\text{R}}^{(j)} = i\alpha(\sigma_{j+}p_{j-}^3 - \sigma_{j-}p_{j+}^3), \quad (2)$$

$$\begin{aligned} \hat{H}_{\text{D}}^{(j)} = & -\beta_3(\sigma_{j+}p_{j-} - p_{j+}p_{j-} + \sigma_{j-}p_{j+} - p_{j-}p_{j+}) \\ & - \beta_1(\sigma_{j+}p_{j-} + \sigma_{j-}p_{j+}). \end{aligned} \quad (3)$$

Here  $\alpha$  ( $\beta_{1,3}$ ) is the Rashba (linear and cubic Dresselhaus) coupling strength.

### A. Spin-orbit tunneling direction

Tunneling may arise from spin-preserving and spin-flip processes. The former corresponds to the interdot tunneling strength  $t_0^{nm} \equiv \langle ^L n_x, n_y | \hat{H}_d^{(L)} | m_x, m_y^R \rangle$ . Similarly, we have for the SOC  $\langle ^L n_x, n_y | \hat{H}_{\text{SO}}^{(L)} | m_x, m_y^R \rangle$ , causing a preferential direction in the spin Hilbert space, which we shall refer to as the tunneling field direction [47,69]. When  $\mathbf{B}$  points along the tunneling field direction, there is no SO tunneling. For the double dot aligned along  $\hat{x}$ , if  $n_y = m_y$ , the Rashba tunneling field is along  $\hat{y}$ , and linear and cubic Dresselhaus tunneling fields both point along  $\hat{x}$ .

### B. Effective tunneling Hamiltonian

The usual PSB involves the (0,2) singlet  $|S_{02}\rangle$ , and the (1,1) states  $\{|S\rangle, |T_0\rangle, |T_{\pm}\rangle\}$ . The expression of the SO couplings between  $|S_{02}\rangle$  and the triplet states can be found in Appendix B. As  $\mathbf{B}$  is rotated, the tunneling matrix elements  $\Delta_0 = \sqrt{2}(it_R \sin \theta + it_D \cos \theta - t_B \cos 2\theta)$  between  $|S_{02}\rangle$  and  $|T_0\rangle$ , and  $\Delta_{\pm} = (t_R \cos \theta - t_D \sin \theta - it_B \sin 2\theta)$  between  $|S_{02}\rangle$  and  $|T_{\pm}\rangle$  will vary in strength. Here we have used  $t_R \equiv \langle ^L 0, 0 | \hat{H}_{\text{R}} | 0, 0^R \rangle$ ,  $t_D \equiv \langle ^L 0, 0 | \hat{H}_{\text{D}} | 0, 0^R \rangle$ ,  $t_B \equiv$

TABLE I. The values of  $t_0$  and  $t_R$  based on the calculated  $\alpha$  for accumulation (A) and inversion (I) layers [68]. For Si there is a significant anisotropic Rashba contribution in  $k_{\parallel}$ , and for hole densities  $\sim 10^{16} \text{ m}^{-2}$ , the ratio of the Rashba spin splitting to the Fermi energy is roughly 0.1, hence  $t_R \sim t_0/10$ .

	GaAs	InAs	InSb	Si
$R_0$ (nm)	30	38	50	20
$t_0$ ( $\mu\text{eV}$ )	230	180	97	530
$\alpha$ ( $\text{meV m}^3$ )	$5.4 \times 10^{-25}$	$3.6 \times 10^{-24}$	$1.0 \times 10^{-23}$	–
$t_R$ ( $\mu\text{eV}$ )	150(A)/50(I)	390(I)	603(I)	–

$f\mu_B B \chi / R_0^2$ , and the orbital overlap  $\chi \equiv \langle {}^L0,0|0,0^R \rangle = e^{-d^2/R_0^2}$ . Because  $|S\rangle$  and  $|T_0\rangle$  are degenerate, we adopt their superpositions  $|M\rangle \equiv \frac{1}{N_M} [\Delta_0^* |S\rangle - t_0 |T_0\rangle]$  and  $|M_{\perp}\rangle \equiv \frac{1}{N_M} (t_0 |S\rangle + \Delta_0 |T_0\rangle)$ , with  $t_0 \equiv t_0^{00}$  and  $N_M = \sqrt{|\Delta_0|^2 + t_0^2}$ .

In the  $\{S_{02}, M, M_{\perp}, T_+, T_-\}$  basis, the effective tunneling Hamiltonian is

$$\hat{H}_{\text{eff}} = \begin{pmatrix} -\epsilon & 0 & N_M & \Delta_+ & \Delta_- \\ 0 & 0 & 0 & 0 & 0 \\ N_M & 0 & 0 & 0 & 0 \\ \Delta_+^* & 0 & 0 & E_Z & 0 \\ \Delta_-^* & 0 & 0 & 0 & -E_Z \end{pmatrix}, \quad (4)$$

with  $\epsilon$  the detuning between (0,2) and (1,1). From Eq. (4), if the two HHs are initialized in  $|M\rangle$ , there will be no leakage without (1,1) spin relaxation. Experimentally, the initial state is often unknown, and there may exist the (1,1) relaxation process.

The effective SO tunneling elements  $\Delta_{0,\pm}$  and  $N_M$  contain terms conditioned by  $t_R$ ,  $t_D$ ,  $t_0$ , and  $t_B$ .  $t_B$  is subject to the HH-LH splitting,  $R$  and  $B$ , and its magnitude, typically is on the order of  $0.1\text{--}1 \mu\text{eV}$  at  $B = 1 \text{ T}$  for GaAs (cf. Appendix A). We expect  $t_R \gg t_D$  [68], and thus calculate the values of  $t_0$  and  $t_R$  for typical semiconductors in Table I.  $R_0$  is chosen so that the HH-LH mixture is a perturbation. We have assumed a small interdot distance such that  $\chi \approx e^{-1}$ , and note that in GaAs,  $t_R/t_0$  for holes may be much higher than for electrons [44]. Based on the above, we can describe the  $\theta$  influence in the typical  $\Delta_{0,\pm}$  and  $N_M$  mainly by considering  $t_R$  and  $t_0$ .

### C. The effective singlet-triplet exchange

Equation (4) may provide insight of the effective singlet-triplet exchange for hole qubits. The basis adopted here can be rotated to the conventional basis used for the singlet-triplet qubit [61], where the pseudospin  $S_z = 0$  subspace (comprised of  $|S_{02}\rangle$ ,  $|M\rangle$ , and  $|M_{\perp}\rangle$ ) is better described by the two charge-spin hybridized singlet states [having the energies of  $E_{S_{\pm}} = (-\epsilon \pm \sqrt{\epsilon^2 + 4t_0^2})/2$ ] and the unpolarized triplet. If the SOC is strong, almost all the two-(pseudo)spin states have the characteristics of both the singlet and triplet, and operating the singlet-triplet qubit requires a fast control to avoid information leakage to the polarized triplet states via the spin relaxation (see later discussion for the relaxation.) Considering the qubit is away from the singlet-triplet anticrossing (i.e., large  $|E_{S_{\pm}} - E_Z|$ ), we obtain the effective singlet-triplet exchange  $J_{\text{ex}}$  by diagonalizing the subspace comprising  $|S_{02}\rangle$ ,

$|S_{11}\rangle$ , and  $|T_0\rangle$ . For a small  $\epsilon \ll t_0$ ,

$$J_{\text{ex}} \approx \left| -\frac{\epsilon}{2} - \sqrt{t_0^2 + |\Delta_0(\theta)|^2} \right|. \quad (5)$$

Figure 2(a) shows  $J_{\text{ex}}(\epsilon = 0)/t_0$  as a function of  $\theta$  with various Rashba strengths. Given a large  $t_R/t_0$  (see Table I), the change in  $J_{\text{ex}}$  by tuning  $\theta$  can be appreciable, cf. the  $t_R = 3t_0$  and  $t_R = 6t_0$  curves in Fig. 2(a), although the latter two would require rather large Zeeman energies. Experimentally,  $J_{\text{ex}}$  is tuned electrically by  $\epsilon$  or  $t_0$  [70], while the cubic Rashba SOC of hole systems may respond to the gate voltage in an opposite fashion to the linear electron SOC [71]. Here we note that adjusting  $\Delta_0(\theta)$  can be achieved without changing the Rashba strength  $t_R$ .

### III. SPIN-ORBIT INDUCED LEAKAGE

The leakage is determined by a final readout of the tunneling from  $(0,2) \rightarrow (0,1)$ . Charge flow from  $(1,1) \rightarrow (0,2) \rightarrow (0,1)$  is balanced by the transition rates between the seven states, including the  $(1,1)$  relaxation rate  $\Gamma_{11}$ . We compute the leakage by solving a set of steady-state kinetic equations  $d\mathcal{P}/dt = -\mathcal{W}_{\text{out}}\mathcal{P} + \mathcal{W}_{\text{in}}\mathcal{P} = 0$ , where  $\mathcal{P} = \{P_k\}, P_{\uparrow}, P_{\downarrow}\}^T$  is a vector consisting of the probabilities  $P_k$  of being in the eigenstates  $\{|k\rangle\}$  of the Hamiltonian (4) and  $P_{\sigma}$  in  $(0,1)$  with the spin  $\sigma$  (see Appendix C for more details.) The transition rates into and out of each state are contracted in the respective matrices  $\mathcal{W}_{\text{in}}$  and  $\mathcal{W}_{\text{out}}$ . We obtain the leakage current  $I = e\Gamma_{\text{DL}}P_{02}$ , with  $\Gamma_{\text{DL}}$  the dot-lead transition rate and  $P_{02}$  the final probability to end in  $(0,2)$ . The following results are shown for  $\epsilon = 0$  and  $t_R \gg t_D, t_B$ .  $\Gamma_{11} = \Gamma_0$  is first set constant to focus on the SO-induced leakage.

Figure 2(b) shows the leakage  $I(\theta)$  and  $I(B)$  in GaAs, when only the two  $B$ -linear Zeeman couplings are included. The PSB is lifted at  $B \neq 0$  by the Rashba SOC, and  $|dI/dB|$  grows when  $t_R$  is increased. While we have solved for  $I$  numerically, if  $t_R, E_Z < t_0$  and  $\Gamma_{11} = \Gamma_0$ ,  $I(E_Z) \sim e\Gamma_{\text{DL}}P_M\gamma^2[1 - \Lambda^2/(E_Z^2 + \Lambda^2)]$ , with  $\Lambda \equiv \gamma t_0^2/|\Delta_+(\theta)|$ ,  $\gamma^2 = \Gamma_{11}/\Gamma_{\text{DL}}$ , and  $P_M$  is the probability of being in  $|M\rangle$ . In this approximation,  $I(B)$  is a Lorentzian (see Appendix D). In Fig. 2(b), the maximal (minimal)  $I(\theta)$  is found when  $|\Delta_+| \approx (t_R^2 \cos^2 \theta + t_B^2 \sin^2 2\theta)^{1/2}$  reaches its maximum (minimum). In Figs. 3(a) and 3(b), when only the  $B^3$  term contributes to  $E_Z$ , the lifting is insignificant at low  $B$ , and the period of  $I(\theta)$  is  $1/3$  of that in the  $B$ -linear case. In Fig. 3(c), competition of the  $B$ -linear and  $B^3$  couplings yields a beat pattern in  $I(\theta)$  for large  $B$ . Figure 3(d) shows the beat pattern present when a relatively strong  $B$ -linear splitting exists in the left dot and the spin splitting in the right dot is  $\propto B^3$ . This may correspond to the case where the two dots are very different in size.

Now we discuss spin-selective  $\Gamma_{11}$ , applying to most situations where the  $(1,1)$  states are well split. For III-V QDs with a large HH-LH splitting, the major cause of spin relaxation is the SO assisted phonon relaxation [16,17,20,25]. Indeed, the SO effect varies in strength as  $\mathbf{B}$  rotated, however, when  $\hat{H}_{\text{SO}}^{(j)}$  yields multiple sources of SO tunneling, spin mixing is present at all  $\mathbf{B}$ . There are two-spin and single-spin relaxation channels. For QDs with a small SO mixture, including two-spin relaxation is sufficient because the current dot orbital is well decoupled from the others. Such two-spin relaxation requires nonvanishing

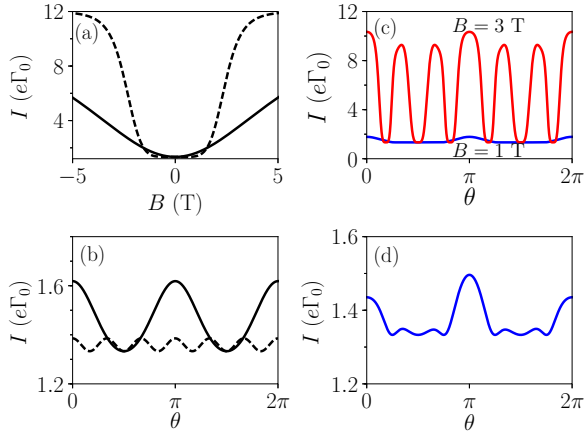


FIG. 3. GaAs double QD with  $R_0 = 80$  nm,  $t_R = 0.5t_0$ , and  $\Gamma_{11} = \Gamma_0 = 3$  MHz. (a)  $I(B)$  with  $\theta = 0$ . The dot-dashed (solid) line is with  $E_Z$  including the only  $B^3$  ( $B$ -linear) term. (b)  $I(\theta)$  at  $B = 1$  T with only the  $B^3$  term (dot-dashed line), and only the  $B$ -linear terms (solid line). (c) The beat pattern in  $I(\theta)$ , when both the  $B^3$  and  $B$ -linear terms included. (d)  $I(\theta)$  at  $B = 1$  T, when the spin splitting in the  $L$  and  $R$  dot is linear and cubic in  $B$ , respectively.

$\Delta_{\pm}(\theta)$ . Otherwise, corrections from single-spin relaxation should be included.

We adopt the  $S-T_{\pm}$  relaxation rate  $\Gamma^{ST_{\pm}}$  and single-spin one  $\Gamma^{\uparrow\downarrow}$ . To compare with the results with  $\Gamma_{11} = \Gamma_0$ , we set  $\Gamma^{ST_{\pm}} \approx \Gamma_0 |\cos \theta|^2$  ( $\Gamma_0 |\cos 3\theta|^2$  in the  $B^3$  case). Assuming the single-spin relaxation assisted by the Dresselhaus SOC, we set  $\Gamma^{\uparrow\downarrow}(B) \propto B^2$  (cf. Appendix E) with  $\Gamma^{\uparrow\downarrow}(B) = \Gamma_0$  at  $B = 1$  T  $\hat{y}$  and vanishes when  $B \parallel \hat{x}$ . In Figs. 4(a) and 4(c), the  $I(B)$  profile shrinks, due to the reduced number of the relaxation channels, while  $I(\theta)$  in Figs. 4(b) and 4(d) have a larger amplitude, from the anisotropic  $\Gamma_{11}$ .

#### IV. EXPERIMENTAL APPLICABILITY

While a recent LH experiment has observed no clear PSB anisotropy in the in-plane field orientation, our results have

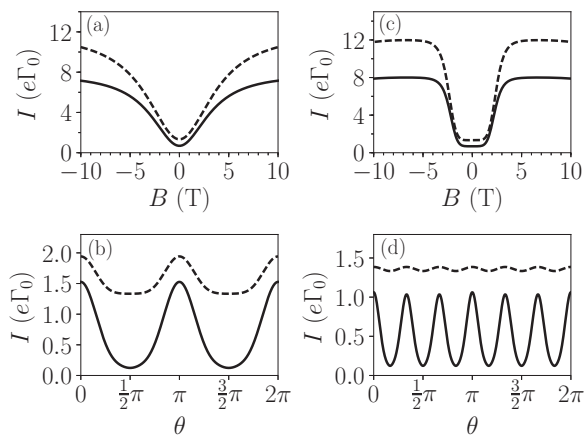


FIG. 4. The leakage  $I(B, \theta)$  with  $t_R = 0.5t_0$  with spin-selective  $\Gamma_{11}$  (solid line) in GaAs. The dashed lines are obtained with a constant  $\Gamma_{11} = \Gamma_0 = 3$  MHz. (a) and (b) At  $R_0 = 30$  nm,  $I(B)$  with  $\theta = 0$  and  $I(\theta)$  at  $B = 1$  T, by the  $B$ -linear terms only. (c) and (d) At  $R_0 = 80$  nm,  $I(B)$  with  $\theta = 0$  and  $I(\theta)$  at  $B = 1$  T, by the  $B^3$  term only.

shown heavy-hole PSB leakage has a dependence of the field orientation and are in agreement with recent experiments [12,13]. We have assumed  $t_R \gg t_D$ , however, if  $t_D \sim t_R$ , their relative strength may be determined by the minimum positions of  $I(\theta)$ . We have focused on the one-hole limit, whereas the existing experiments are often performed with higher charge filling [9,13,14] and the SO tunneling direction is sensitive to the dot shape and the symmetry of involved dot orbitals [13].

The anisotropic  $I(\theta)$  can be manipulated by varying  $\theta$  and employed in probing the power of  $B$  in the Zeeman interaction via the signal period. Because  $\Delta_{\pm}$  may be determined from the singlet-triplet anticrossing (with  $t_0$  extracted from the  $\epsilon = 0$  anticrossing),  $|E_Z|$  can be estimated via  $I(B)$ . Desired  $I(\theta)$  can be engineered for further applications, while we should note that varying the magnetic field orientation can be experimentally challenging in the current state of art.

The other (implicit) contribution to the leakage is from  $\Gamma_{11}$ . We have considered  $\Gamma_{11}$  on the order of MHz, making the calculated  $I$  of several pA [12,13]. Lastly, Ref. [68] shows that the perturbative approach may break down if the hole density reaches a critical value. The current model then requires a lower bound for the dot radius  $R_0$ . Their results of GaAs accumulation (inversion) layers therein suggest  $R_0 \gtrsim 13$  nm ( $\gtrsim 5.6$  nm).

#### V. CONCLUSIONS

We have studied the SO-induced PSB leakage in a two-HH double QD in an in-plane magnetic field. We have shown that the anisotropic leakage signal may be employed as a probe of the Zeeman coupling in hole QDs, and this signal and the singlet-triplet exchange splitting may be controlled by varying the field orientation. We will extend our work with the full  $J = \frac{3}{2}$  Hamiltonian to acquire more complete behavior of confined holes.

#### ACKNOWLEDGMENTS

We thank Daisy Q. Wang for providing experimental data and useful discussion, and Tetsuo Kodera and András Pályi for fruitful discussions. This work is supported by the ARC through the DP scheme.

#### APPENDIX A: THE INDIRECT MAGNETIC COUPLINGS

According to Ref. [66], the parameter  $f = f_1 + f_2$  from the indirect  $B$ -linear coupling has two contributions. The contribution  $f_1$  concerns the HH-LH mixing at the same subband along the  $\hat{z}$  direction, whereas  $f_2$  involves the HH-LH mixing between different  $\hat{z}$  subbands. The overall contribution  $f$  is strongly affected by the confinement asymmetry in 2D hole systems.

Below we consider a quasitriangular well and focus on the first subband  $a = 1$  only ( $f_2 < f_1$  in our case). We estimate  $f_1$  using the Fang-Howard trial wave function  $F_i(z) = 2\lambda_i^{3/2}ze^{-\lambda_i z}$  with  $\lambda_i = \lambda_h$  for HHs and  $\lambda_i = \lambda_l$  for LHs [72]. We obtain

$$f_1 \approx -\frac{3}{2}\kappa\bar{\gamma}\frac{\hbar^2}{m_0(E_1^h - E_1^l)}\frac{128\lambda_h^3\lambda_l^3}{(\lambda_h + \lambda_l)^6}, \quad (\text{A1})$$

with  $m_0$  the free-electron mass and  $E_a^{h(l)}$  the energy of the 2D HH (LH) state  $|h_a(l_a)\rangle$  at the subband  $a$ . We have assumed the axial approximation  $\bar{\gamma} = \frac{1}{2}(\gamma_2 + \gamma_3)$  with  $\gamma_{1,2,3}$  the Luttinger parameters. For typical hole densities  $\sim 10^{15} \text{ m}^{-2}$ , the indirect  $B$ -linear effect corresponding to  $f_1$  is on the order of  $\mu\text{eV}$  at  $B = 1 \text{ T}$  in GaAs.

The other indirect coupling cubic in  $B$  is significant for large QDs and at high fields, and we refer to Eq. (7.19) of Ref. [66] (and its errata) for the expression of  $F$ .

## APPENDIX B: THE SO COUPLING FORM

Here we give the Rashba and cubic Dresselhaus couplings for the two HHs occupying on the ground orbital  $|0,0^{(j)}\rangle = (\pi R_0^2)^{-1} e^{-(x-x_j)^2+y^2/2R_0^2}$ . The spin basis is given the bulk- $q$  Zeeman term

$$\langle S_{02} | \sum_j \hat{H}_R^{(j)} | T_{\pm} \rangle = \pm \frac{\alpha \hbar^3}{R_0^3} \cos \theta e^{-\zeta^2} \zeta^3, \quad (\text{B1})$$

$$\langle S_{02} | \sum_j \hat{H}_R^{(j)} | T_0 \rangle = i \frac{\sqrt{2} \alpha \hbar^3}{R_0^3} \sin \theta e^{-\zeta^2} \zeta^3, \quad (\text{B2})$$

$$\langle S_{02} | \sum_j \hat{H}_D^{(j)} | T_{\pm} \rangle = \mp \frac{\beta_3 \hbar^3}{R_0^3} \sin \theta e^{-\zeta^2} \xi (2 - \zeta^2), \quad (\text{B3})$$

$$\langle S_{02} | \sum_j \hat{H}_D^{(j)} | T_0 \rangle = i \frac{\sqrt{2} \beta_3 \hbar^3}{R_0^3} \cos \theta e^{-\zeta^2} \zeta (2 - \zeta^2), \quad (\text{B4})$$

where  $\zeta \equiv d/R_0$  and  $\chi = e^{-\zeta^2}$  is the orbital overlap.

## APPENDIX C: THE STEADY-STATE KINETIC EQUATIONS

The kinetic equations used in the main text are given by

$$\begin{aligned} \frac{dP_k}{dt} &= \sum_{\sigma} (U_{\sigma k} P_{\sigma} - W_{k\sigma} P_k) + \sum_{k' \neq k} (\Gamma_{k'} P_{k'} - \Gamma_k P_k) = 0, \\ \frac{dP_{\sigma}}{dt} &= \sum_k (W_{k\sigma} P_k - U_{\sigma k} P_{\sigma}) = 0, \end{aligned} \quad (\text{C1})$$

where  $\Gamma_k$  is the (1,1) relaxation rate out of  $|k\rangle$ .  $W_{k\sigma}$  and  $U_{\sigma k}$ , given as follows, correspond to the escape rates from  $|k\rangle$  to  $(0,1)_{\sigma}$  and the refilling rate from  $(0,1)_{\sigma}$  to  $|k\rangle$ :

$$W_{k\sigma} = \Gamma_R \sum_{\sigma'} |\langle (0,1)_{\sigma} | d_{R_{\sigma'}} | k \rangle|^2, \quad (\text{C2})$$

$$U_{\sigma k} = \Gamma_L \sum_{\sigma'} |\langle k | d_{L_{\sigma'}}^+ | (0,1)_{\sigma} \rangle|^2, \quad (\text{C3})$$

with  $\Gamma_{R(L)}$  the tunneling rate between the right (left) dot and lead, and  $d_j(d_j^+)$  the HH annihilation (creation) operator on the  $j$  dot.

## APPENDIX D: SIMPLIFIED EXPRESSIONS OF THE LEAKAGE CURRENT

The leakage current is given by  $I = e\Gamma_R P_{02} = e \sum_{\sigma,k} W_{k\sigma} P_k$ .

When  $B \rightarrow 0$ , only one state  $|u\rangle$  is unblocked, making  $W_{k\sigma} = 0$  for  $k \neq u$ . We have  $P(0,1)_{\sigma} = \sum_k (W_{k\sigma} P_k / U_{\sigma k})$  from Eq. (C1), and write the probability in  $|u\rangle$  by  $P_u =$

$\frac{1}{3\Gamma_u} \sum_{k \neq u} \Gamma_k P_k$ . The resulting current becomes  $I(B \rightarrow 0) = \sum_{\sigma, k \neq u} \frac{e W_{u\sigma}}{3\Gamma_u} \Gamma_k P_k$ . We note that  $I(B \rightarrow 0)$  is only nonzero due to a finite (1,1) relaxation rate  $\Gamma_k$ . For a rough estimate, we assume that  $|u\rangle$  contains the amplitude  $A_{u,02}$  of  $|S_{02}\rangle$  so that  $W_{u\sigma} = \frac{\Gamma_R}{2} |A_{u,02}|^2$ , and obtain  $I_0 \sim e\Gamma_{\text{DL}} \frac{|A_{u,02}|^2}{3} \sum_{k \neq u} P_k$ , with  $\Gamma_{\text{DL}} \sim \Gamma_{L(R)}$  and  $\Gamma_{u,k} \sim \Gamma_{11}$ .

For  $B \neq 0$ , the probability in an unblocked state  $|u\rangle$  is  $P_u = P_M \sum_{\sigma} [\Gamma_M U_{\sigma u} (\Gamma_u U_{\sigma u} + 2W_{\sigma M} W_{u\sigma})^{-1}]$ . This leads to a leakage current

$$I = e P_M \sum_{u,\sigma} W_{u\sigma} \sum_{\sigma'} \frac{\Gamma_M U_{\sigma'u}}{\Gamma_u U_{\sigma'u} + 2U_{\sigma M} W_{u\sigma'}}.$$

For a rough estimate, we find

$$I \sim e\Gamma_{\text{DL}} P_M \sum_u \frac{|A_{u,02}|^2 |A_{u,11}|^2 \gamma^2}{|A_{u,11}|^2 \gamma^2 + |A_{u,02}|^2}, \quad (\text{D1})$$

where  $\gamma^2 \equiv \Gamma_{11}/\Gamma_{\text{DL}}$  and  $U_{\sigma u} \equiv \frac{\Gamma_R}{2} |A_{u,11}|^2$  with  $A_{u,11}$  the amplitude of the (1,1) charge configuration in  $|u\rangle$ . At  $\epsilon = 0$ , when the SO coupling is a perturbation to a large  $t_0 > E_Z$ , we have  $A_{T_{\pm},02} \propto |\Delta_{\pm}| E_Z (E_Z^2 - t_0^2)^{-1}$  and  $A_{T_{\pm},11}$  barely depends on  $E_Z$ . As such, the leakage current  $I \sim e\Gamma_{\text{DL}} P_M E_Z^2 \gamma^2 (E_Z^2 + \frac{t_0^4}{|\Delta_{\pm}|^2} \gamma^2)^{-1}$  when  $|E_Z|/t_0$  is small. This approximated  $I(B)$  has a Lorentzian shape [43].

## APPENDIX E: THE PHONON INDUCED RELAXATION

The hole-phonon interaction is [17,20,25,73]

$$\dot{H}_{\text{ph}} = \sum_{q\lambda} \frac{F(q_z) e^{i\mathbf{q}_{\parallel} \cdot (\mathbf{r}_1 + \mathbf{r}_2)}}{\sqrt{2\rho_c \omega_{q\lambda} / \hbar^2}} [P(\mathbf{q}) - iD(\mathbf{q})] (b_{-\mathbf{q}\lambda}^+ + b_{\mathbf{q}\lambda}), \quad (\text{E1})$$

where  $P(\mathbf{q}) = e\beta_{\mathbf{q}\lambda}$  and  $D(\mathbf{q}) = (D_0 \mathbf{q} \cdot \boldsymbol{\xi}_{q\lambda} - D_z q_z \xi_{q\lambda}^z)$  result from the piezoelectric field  $\beta_{\mathbf{q}\lambda}$  and deformation  $D_{0/z}$ . We have denoted by  $\xi_{q\lambda}$  at the wave number  $q$  and the vibration mode  $\lambda$ , by  $b_{\mathbf{q}\lambda}^+$  ( $b_{\mathbf{q}\lambda}$ ) phonon creation (annihilation) operator, and by  $\rho_c$  the crystal mass density. The factor  $F(q_z)$  is a unity within the dot height, otherwise it is vanishing.

The hole-phonon interaction couples the double-dot orbitals through the phase factor  $e^{i\mathbf{q}_{\parallel} \cdot (\mathbf{r}_1 + \mathbf{r}_2)}$ . For QD qubits, the dipole approximation  $e^{i\mathbf{q}_{\parallel} \cdot (\mathbf{r}_1 + \mathbf{r}_2)} \approx 1 + i\mathbf{q}_{\parallel} \cdot (\mathbf{r}_1 + \mathbf{r}_2)$  is reasonable [74] and yields analytic results. Within the approximation, the piezoelectric coupling ( $\propto 1/\sqrt{q}$ ) is the dominant phonon relaxation mechanism.

For the singlet-triplet relaxation, the effective  $S_{11}$  and  $T_-$  are given by  $|S'_{11}\rangle = a|S_{11}\rangle + c_+|T_+\rangle + c_-|T_-\rangle$  and  $|T'_-\rangle = b|S_{11}\rangle + d_-|T_-\rangle$  with appropriate state coefficients  $a, b, c_+, c_-$ , and  $d_-$ . The effective  $S_{11}-T_-$  relaxation rate due to the piezoelectric coupling is given by  $\Gamma_{\lambda}^{\text{ST-}} = (|a^*b|^2 + |c_-^*d_-|^2) \Gamma_{\lambda}^{\text{PE,ST}}$ , where the base rate

$$\Gamma_{\lambda}^{\text{PE,ST}} \approx \eta_{\lambda}^{\text{PE}} \frac{2(eh_{14})^2}{\hbar \rho_c \epsilon_r^2 v_{\lambda}^3} \omega_{\text{ST}} [1 + n(\omega_{\text{ST}})], \quad (\text{E2})$$

with  $eh_{14} = 1.2 \times 10^9 \text{ V/m}$ ,  $\epsilon_r$  is the relative permittivity,  $\hbar \omega_{\text{ST}}$  is the singlet-triplet energy separation, and  $v_{\lambda} = v_{l(t)}$  is the longitudinal (transverse) acoustic speed. The dimensionless parameters  $\{\eta_{\lambda}^{\text{PE}}, \eta_{t1}^{\text{PE}}, \eta_{t2}^{\text{PE}}\} = \{\frac{12}{5}, \frac{4}{21}, \frac{1}{15}\}$  are obtained for the longitudinal and two transverse phonons, respectively. For

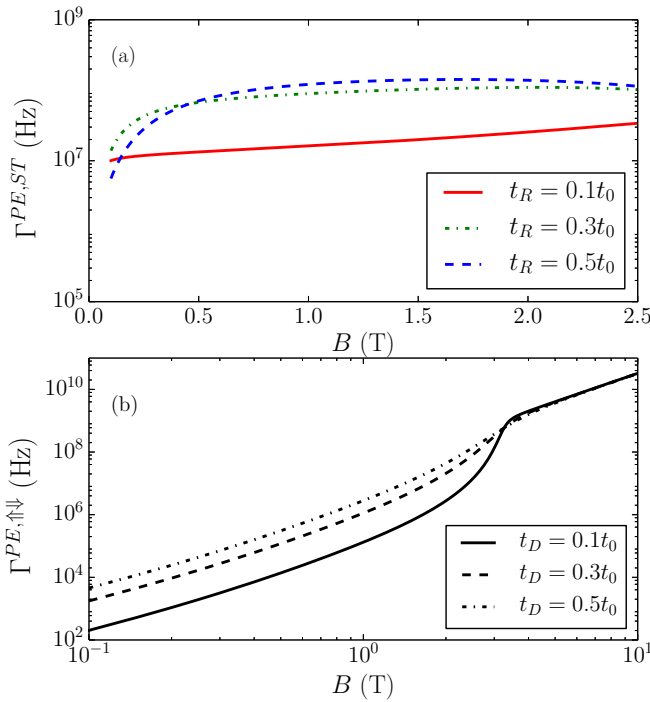


FIG. 5. (a) The Rashba-assisted singlet-triplet relaxation rate due to piezoelectric phonons as a function of  $B$ . (b) The Dresselhaus-assisted single-spin relaxation rate as a function of  $B$ , when the first three excited orbitals are included.  $t_0 = 200 \mu\text{eV}$ . The 2D confinement given by  $R_0 = 30 \text{ nm}$  is about  $190 \mu\text{eV}$ . The curves in (b) meet when  $B \gtrsim 3 \text{ T}$  as  $|E_Z| \rightarrow t_0$  (i.e., the singlet-triplet crossing).

completeness, the singlet-triplet base rate due to deformation phonons is given by

$$\Gamma_{\lambda}^{\text{DP},\text{ST}} \approx \eta_{\lambda}^{\text{DP}} \frac{\omega_Z^3}{\pi^2 \hbar \rho_c v_{\lambda}^5} [1 + n(\omega_Z)], \quad (\text{E3})$$

- [1] D. Brunner, B. D. Gerardot, P. A. Dalgarno, G. Wüst, K. Karrai, N. G. Stoltz, P. M. Petroff, and R. J. Warburton, *Science* **325**, 70 (2009).
- [2] F. A. Zwanenburg, C. E. W. M. Van Rijmenam, Y. Fang, C. M. Lieber, and L. P. Kouwenhoven, *Nano Lett.* **9**, 1071 (2009).
- [3] K. De Greve, P. L. McMahon, D. Press, T. D. Ladd, D. Bisping, C. Schneider, M. Kamp, L. Worschech, S. Hofling, A. Forchel *et al.*, *Nat. Phys.* **7**, 872 (2011).
- [4] A. Greilich, S. G. Carter, D. Kim, A. S. Bracker, and D. Gammon, *Nat. Photon.* **5**, 702 (2011).
- [5] P. C. Spruijtenburg, J. Ridderbos, F. Mueller, A. W. Leenstra, M. Brauns, A. A. I. Aarnink, W. G. Van Der Wiel, and F. A. Zwanenburg, *Appl. Phys. Lett.* **102**, 192105 (2013).
- [6] R. Li, F. E. Hudson, A. S. Dzurak, and A. R. Hamilton, *Appl. Phys. Lett.* **103**, 163508 (2013).
- [7] V. S. Pribiag, S. Nadj-Perge, S. M. Frolov, J. W. G. van den Berg, I. van Weperen, S. R. Plissard, E. P. A. M. Bakkers, and L. P. Kouwenhoven, *Nat. Nano* **8**, 170 (2013).
- [8] F. Mueller, G. Konstantaras, W. G. Van Der Wiel, and F. A. Zwanenburg, *Appl. Phys. Lett.* **106**, 172101 (2015).
- [9] R. Li, F. E. Hudson, A. S. Dzurak, and A. R. Hamilton, *Nano Lett.* **15**, 7314 (2015).
- [10] B. Voisin, R. Maurand, S. Barraud, M. Vinet, X. Jehl, M. Sanquer, J. Renard, and S. De Franceschi, *Nano Lett.* **16**, 88 (2016).
- [11] M. Brauns, J. Ridderbos, A. Li, E. P. A. M. Bakkers, and F. A. Zwanenburg, *Phys. Rev. B* **93**, 121408 (2016).
- [12] M. Brauns, J. Ridderbos, A. Li, E. P. A. M. Bakkers, W. G. van der Wiel, and F. A. Zwanenburg, *Phys. Rev. B* **94**, 041411 (2016).
- [13] D. Q. Wang, O. Klochan, J.-T. Hung, D. Culcer, I. Farrer, A. R. David, and A. R. Hamilton, *Nano Lett.* **16**, 7685 (2016).
- [14] H. Bohuslavskyi, D. Kotekar-Patil, R. Maurand, A. Corra, S. Barraud, L. Bourdet, L. Hutin, Y.-M. Niquet, X. Jehl, S. De Franceschi, M. Vinet, and M. Sanquer, *Appl. Phys. Lett.* **109**, 193101 (2016).
- [15] A. Zarassi, Z. Su, J. Danon, J. Schwenderling, M. Hocevar, B. M. Nguyen, J. Yoo, S. A. Dayeh, and S. M. Frolov, *Phys. Rev. B* **95**, 155416 (2017).
- [16] L. M. Woods, T. L. Reinecke, and Y. Lyanda-Geller, *Phys. Rev. B* **66**, 161318(R) (2002).
- [17] D. V. Bulaev and D. Loss, *Phys. Rev. Lett.* **95**, 076805 (2005).
- [18] D. V. Bulaev and D. Loss, *Phys. Rev. Lett.* **98**, 097202 (2007).
- [19] J. Fischer, W. A. Coish, D. V. Bulaev, and D. Loss, *Phys. Rev. B* **78**, 155329 (2008).

where  $\{\eta_l^{\text{DP}}, \eta_{t1}^{\text{DP}}, \eta_{t2}^{\text{DP}}\} = \{\frac{(2D_a^2+D_b^2)}{4}, \frac{D_b^2}{140}, 0\}$  with  $D_a = 1.16 \text{ eV}$  and  $D_b = -2.0 \text{ eV}$  for GaAs [25].

When the SO mixture is large enough, corrections from single-spin relaxation channels should be included. The Rashba interaction  $\hat{H}_{\text{R}}^{(j)} \propto p_j^3$  couples the ground orbital to the third excited orbital and so on, whereas the Dresselhaus interaction couples the ground orbital to all the others directly or indirectly. For example, the effective left spin states  $|\uparrow\rangle$  and  $|\downarrow\rangle$  due to the Dresselhaus interaction are given by  $|\uparrow\rangle = \sum_{\sigma} a_{\sigma,0} |\sigma\rangle |0,0\rangle + \sum_{n',\sigma} a_{\sigma,n'} |\sigma\rangle |n'_x, n'_y\rangle$  and  $|\downarrow\rangle = \sum_{\sigma} b_{\sigma,0} |\sigma\rangle |0,0\rangle + \sum_{n',\sigma} b_{\sigma,n'} |\sigma\rangle |n'_x, n'_y\rangle$ , where  $n' = \{n'_x, n'_y\} \neq \{0,0\}$  includes all the excited orbitals, and  $a_{\sigma,n}$  and  $b_{\sigma,n}$  are the coefficients of the  $|\uparrow\rangle$  and  $|\downarrow\rangle$ , with the corresponding spin  $\sigma$  and orbital indices  $n$ . In this case, the piezoelectric-phonon relaxation rate is given by  $\Gamma^{\uparrow\downarrow} = \sum_{n'} (|a_{\uparrow,0}^* b_{\downarrow,n'}|^2 + |b_{\downarrow,0}^* a_{\uparrow,n'}|^2) \Gamma_{\lambda}^{\text{PE}}$ , where the base rate

$$\Gamma_{\lambda}^{\text{PE},\uparrow\downarrow} \approx \gamma_{\lambda}^{\text{PE}} \frac{(e h_{14})^2 R_0^2}{\hbar \rho_c \epsilon_r^2 v_{\lambda}^5} \omega_Z^3 [1 + n(\omega_Z)], \quad (\text{E4})$$

with  $\{\gamma_l^{\text{PE}}, \gamma_{t1}^{\text{PE}}, \gamma_{t2}^{\text{PE}}\} = \{\frac{4}{35}, \frac{8}{105}, \frac{32}{1155}\}$  and  $\omega_Z = E_Z/\hbar$ .

In Fig. 5 we plot  $\Gamma^{\text{PE},\text{ST}}$  and  $\Gamma^{\text{PE},\uparrow\downarrow}$  to show the field dependence in the relaxation rate. For the  $\Gamma^{\text{PE},\uparrow\downarrow}$  plot, we include only the first three excited orbitals and the actual rate may be more enhanced. The base rate due to deformation is given by

$$\Gamma_{\lambda}^{\text{DP},\uparrow\downarrow} \approx \gamma_{\lambda}^{\text{DP}} \frac{R_0^2 \omega_Z^5}{\pi^2 \hbar \rho_c v_{\lambda}^7} [1 + n(\omega_Z)], \quad (\text{E5})$$

where  $\{\gamma_l^{\text{DP}}, \gamma_{t1}^{\text{DP}}, \gamma_{t2}^{\text{DP}}\} = \{\frac{(7D_a^2+D_b^2)}{84}, \frac{D_b^2}{105}, 0\}$ .

- [20] M. Trif, P. Simon, and D. Loss, *Phys. Rev. Lett.* **103**, 106601 (2009).
- [21] J. Fischer and D. Loss, *Phys. Rev. Lett.* **105**, 266603 (2010).
- [22] X. J. Wang, S. Chesi, and W. A. Coish, *Phys. Rev. Lett.* **109**, 237601 (2012).
- [23] P. Szumniak, S. Bednarek, J. Pawłowski, and B. Partoens, *Phys. Rev. B* **87**, 195307 (2013).
- [24] F. Maier, C. Kloeffel, and D. Loss, *Phys. Rev. B* **87**, 161305 (2013).
- [25] J. I. Climente, C. Segarra, and J. Planelles, *New J. Phys.* **15**, 093009 (2013).
- [26] J. Luttinger and W. Kohn, *Phys. Rev.* **97**, 869 (1955).
- [27] J. Luttinger, *Phys. Rev.* **102**, 1030 (1956).
- [28] R. Winkler, D. Culcer, S. J. Papadakis, B. Habib, and M. Shayegan, *Semicond. Sci. Technol.* **23**, 114017 (2008).
- [29] D. Culcer, C. Lechner, and R. Winkler, *Phys. Rev. Lett.* **97**, 106601 (2006).
- [30] D. Culcer and R. Winkler, *Phys. Rev. Lett.* **99**, 226601 (2007).
- [31] T. Kernreiter, M. Governale, R. Winkler, and U. Zülicke, *Phys. Rev. B* **88**, 125309 (2013).
- [32] C. Kloeffel and D. Loss, *Annu. Rev. Condens. Matter Phys.* **4**, 51 (2013).
- [33] C. Y. Hsieh, R. Cheriton, M. Korkusinski, and P. Hawrylak, *Phys. Rev. B* **80**, 235320 (2009).
- [34] J. Salfi, M. Tong, S. Rogge, and D. Culcer, *Nanotechnology* **27**, 244001 (2016).
- [35] J. Salfi, J. A. Mol, D. Culcer, and S. Rogge, *Phys. Rev. Lett.* **116**, 246801 (2016).
- [36] L. Mao, M. Gong, E. Dumitrescu, S. Tewari, and C. Zhang, *Phys. Rev. Lett.* **108**, 177001 (2012).
- [37] F. Maier, J. Klinovaja, and D. Loss, *Phys. Rev. B* **90**, 195421 (2014).
- [38] J. Liang and Y. Lyanda-Geller, *arXiv:1603.03750*.
- [39] D. Hsieh, Y. Xia, D. Qian, L. Wray, J. D. Dil, F. Meier, J. Osterwalder, L. Patthey, J. G. Checkelsky, N. P. Ong *et al.*, *Nature (London)* **460**, 1101 (2009).
- [40] L. Nádvorník, M. Orlita, N. A. Goncharuk, L. Smrčka, V. Novák, V. Jurka, K. Hruška, Z. Výborný, Z. R. Wasilewski, M. Potemski *et al.*, *New J. Phys.* **14**, 053002 (2012).
- [41] M. Polini, F. Guinea, M. Lewenstein, H. C. Manoharan, and V. Pellegrini, *Nat. Nanotech.* **8**, 625 (2013).
- [42] K. Ono, D. G. Austing, Y. Tokura, and S. Tarucha, *Science* **297**, 1313 (2002).
- [43] J. Danon and Y. V. Nazarov, *Phys. Rev. B* **80**, 041301 (2009).
- [44] S. Nadj-Perge, S. M. Frolov, J. W. W. van Tilburg, J. Danon, Y. V. Nazarov, R. Algra, E. P. A. M. Bakkers, and L. P. Kouwenhoven, *Phys. Rev. B* **81**, 201305 (2010).
- [45] T. Fujita, P. Stano, G. Allison, K. Morimoto, Y. Sato, M. Larsson, J. H. Park, A. Ludwig, A. D. Wieck, A. Oiwa *et al.*, *Phys. Rev. Lett.* **117**, 206802 (2016).
- [46] R. Hanson, L. P. Kouwenhoven, J. R. Petta, S. Tarucha, and L. M. K. Vandersypen, *Rev. Mod. Phys.* **79**, 1217 (2007).
- [47] S. Nadj-Perge, V. S. Pribiag, J. W. G. van den Berg, K. Zuo, S. R. Plissard, E. P. A. M. Bakkers, S. M. Frolov, and L. P. Kouwenhoven, *Phys. Rev. Lett.* **108**, 166801 (2012).
- [48] R. Winkler, S. J. Papadakis, E. P. De Poortere, and M. Shayegan, *Phys. Rev. Lett.* **85**, 4574 (2000).
- [49] R. Winkler, H. Noh, E. Tutuc, and M. Shayegan, *Phys. Rev. B* **65**, 155303 (2002).
- [50] A. Y. Silov, P. A. Blajnov, J. H. Wolter, R. Hey, K. H. Ploog, and N. S. Averkiev, *Appl. Phys. Lett.* **85**, 5929 (2004).
- [51] M. W. Wu, J. H. Jiang, and M. Q. Weng, *Phys. Rep.* **493**, 61 (2010).
- [52] F. Nichele, A. N. Pal, R. Winkler, C. Gerl, W. Wegscheider, T. Ihn, and K. Ensslin, *Phys. Rev. B* **89**, 081306 (2014).
- [53] M. V. Durnev, M. M. Glazov, and E. L. Ivchenko, *Phys. Rev. B* **89**, 075430 (2014).
- [54] P. Wenk, M. Kammermeier, and J. Schliemann, *Phys. Rev. B* **93**, 115312 (2016).
- [55] S. I. Dorozhkin, *Phys. Rev. B* **61**, 7803 (2000).
- [56] X. Marie, T. Amand, P. Le Jeune, M. Paillard, P. Renucci, L. E. Golub, V. D. Dymnikov, and E. L. Ivchenko, *Phys. Rev. B* **60**, 5811 (1999).
- [57] M. Rahimi, M. R. Sakr, S. V. Kravchenko, S. C. Dultz, and H. W. Jiang, *Phys. Rev. B* **67**, 081302 (2003).
- [58] Z. Q. Yuan, R. R. Du, M. J. Manfra, L. N. Pfeiffer, and K. W. West, *Appl. Phys. Lett.* **94**, 052103 (2009).
- [59] E. Marcellina *et al.* (in preparation).
- [60] D. Loss and D. P. DiVincenzo, *Phys. Rev. A* **57**, 120 (1998).
- [61] J. R. Petta, A. C. Johnson, J. M. Taylor, E. A. Laird, A. Yacoby, M. D. Lukin, C. M. Marcus, M. P. Hanson, and A. C. Gossard, *Science* **309**, 2180 (2005).
- [62] J. J. Pla, K. Y. Tan, J. P. Dehollain, W. H. Lim, J. J. L. Morton, D. N. Jamieson, A. S. Dzurak, and A. Morello, *Nature (London)* **489**, 541 (2012).
- [63] Z. Shi, C. B. Simmons, J. R. Prance, J. K. Gamble, T. S. Koh, Y.-P. Shim, X. Hu, D. E. Savage, M. G. Lagally, M. A. Eriksson *et al.*, *Phys. Rev. Lett.* **108**, 140503 (2012).
- [64] J. Medford, J. Beil, J. M. Taylor, S. D. Bartlett, A. C. Doherty, E. I. Rashba, D. P. DiVincenzo, H. Lu, A. C. Gossard, and C. M. Marcus, *Nat. Nanotech.* **8**, 654 (2013).
- [65] J. Medford, J. Beil, J. M. Taylor, E. I. Rashba, H. Lu, A. C. Gossard, and C. M. Marcus, *Phys. Rev. Lett.* **111**, 050501 (2013).
- [66] R. Winkler, *Spin-Orbit Coupling Effects in Two-Dimensional Electron and Hole Systems* (Springer, Berlin, 2003).
- [67] C. E. Pryor and M. E. Flatte, *Phys. Rev. Lett.* **96**, 026804 (2006).
- [68] E. Marcellina, A. R. Hamilton, R. Winkler, and D. Culcer, *Phys. Rev. B* **95**, 075305 (2017).
- [69] S. Takahashi, R. S. Deacon, K. Yoshida, A. Oiwa, K. Shibata, K. Hirakawa, Y. Tokura, and S. Tarucha, *Phys. Rev. Lett.* **104**, 246801 (2010).
- [70] T. Kodera (private communication).
- [71] B. Habib, E. Tutuc, S. Melinte, M. Shayegan, D. Wasserman, S. A. Lyon, and R. Winkler, *Appl. Phys. Lett.* **85**, 3151 (2004).
- [72] J. H. Davies, *The Physics of Low-dimensional Semiconductors* (Cambridge University Press, Cambridge, 1998).
- [73] L. M. Woods, T. L. Reinecke, and R. Kotlyar, *Phys. Rev. B* **69**, 125330 (2004).
- [74] P. Huang and X. Hu, *Phys. Rev. B* **90**, 235315 (2014).